

SINGLE-KNOB BEAM LINE FOR TRANSVERSE EMITTANCE PARTITIONING

C. Xiao, L. Groening, O.K Kester, H. Leibrock, M. Maier, and P. Rottländer,
GSI, Darmstadt, Germany

M. Chung, Ulsan National Institute of Science and Technology, Ulsan, Republic of Korea

Abstract

Flat beams feature unequal emittances in the horizontal and vertical phase space. Such beams were created successfully in electron machines by applying effective stand-alone solenoid fringe fields in the electron gun. Extension of this method to ion beams was proposed conceptually. This contribution is on the decoupling capabilities of an ion beam emittance transfer line. The proposed beam line provides a single-knob-tool to partition the horizontal and vertical rms emittances, while keeping the product of the two emittances constant as well as the transverse rms Twiss parameters ($\alpha_{x,y}$ and $\beta_{x,y}$) in both planes. It is shown that this single knob is the solenoid field strength, and now we fully understand the decoupling features.

INTRODUCTION

Beams provided from linear accelerator are generally round, and the horizontal and vertical emittances are quite equal. However, the transverse acceptance of subsequent rings might be flat. For instance, the multi-turn injection schemes using orbit bumps in one plane impose flat injection acceptances. Round-to-flat transformation requires a change of the beam eigen-emittances by a non-symplectic transformation [1].

Such a transformation can be performed by placing a charge state stripper inside a longitudinal field region as proposed in [2]. Inside such a solenoidal stripper, the transverse inter-plane correlations are created non-symplectically. Afterwards they are removed symplectically with three skew quadrupoles. A set-up providing round-to-flat transformation is shown in Fig. 1. Such a solenoidal stripper is proposed to be integrated into the existing charge state stripping and separating beam line of the GSI UNILAC [3].

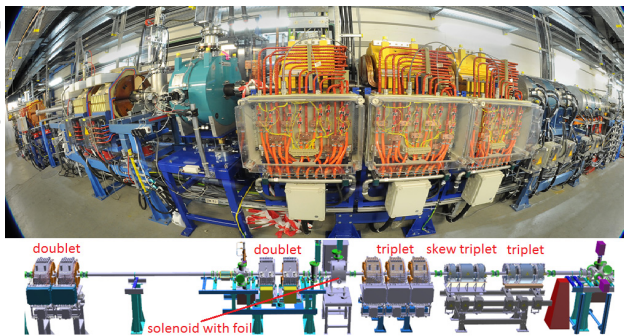


Figure 1: Emittance transfer experiment (EMTEX) beam line for demonstration of transverse rms emittance transfer.

BASIC MATHEMATICAL FOUNDATION

The four-dimensional symmetric beam matrix

$$C = \begin{bmatrix} \langle xx \rangle & \langle xx' \rangle & \langle xy \rangle & \langle xy' \rangle \\ \langle x'x \rangle & \langle x'x' \rangle & \langle x'y \rangle & \langle x'y' \rangle \\ \langle yx \rangle & \langle yx' \rangle & \langle yy \rangle & \langle yy' \rangle \\ \langle y'x \rangle & \langle y'x' \rangle & \langle y'y \rangle & \langle y'y' \rangle \end{bmatrix}. \quad (1)$$

contains ten unique elements, four of which describe the coupling. If at least one of the elements of the off-diagonal sub-matrix is non-zero, the beam is x - y coupled. The four-dimensional rms emittance ε_{4d} is the square root of the determinant of C , and the projected beam rms emittances ε_x and ε_y are the square roots of the determinants of the on-diagonal sub-matrices. Diagonalization of the beam matrix yields the eigen-emittances ε_1 and ε_2 , and the transverse eigen-emittances are calculated as [4]:

$$\varepsilon_1 = \frac{1}{2} \sqrt{-\text{tr}[(CJ)^2] - \sqrt{\text{tr}^2[(CJ)^2] - 16|C|}}, \quad (2)$$

$$\varepsilon_2 = \frac{1}{2} \sqrt{-\text{tr}[(CJ)^2] + \sqrt{\text{tr}^2[(CJ)^2] - 16|C|}}. \quad (3)$$

The four-dimensional matrix J is the skew-symmetric matrix with non-zero entries on the block diagonal of form:

$$J = \begin{bmatrix} 0 & 1 & 0 & 0 \\ -1 & 0 & 0 & 0 \\ 0 & 0 & 0 & 1 \\ 0 & 0 & -1 & 0 \end{bmatrix}. \quad (4)$$

Any symplectic transformation M obeys

$$M^T J M = J. \quad (5)$$

Eigen-emittances are invariant under symplectic transformations, and the transverse eigen-emittances are equal to the transverse rms emittances when inter-plane correlations are zero.

STRIPPING INSIDE A SOLENOID

Stripping inside a solenoid is fundamentally different from stripping between two solenoids due to the longitudinal magnetic field component and the fringe fields. In case of pure transverse field components (dipoles, quadrupoles, n-poles) there is equivalence between stripping inside this magnet and stripping between two such magnets of half lengths.

Let C_0 denote the second moment matrix at the entrance of the solenoid. If the beam has equal horizontal and vertical rms emittances and no inter-plane correlations, the beam matrix can be simplified to (in the case here, $\alpha_{x,y}=0$)

$$C_0 = \begin{bmatrix} \varepsilon\beta & 0 & 0 & 0 \\ 0 & \frac{\varepsilon}{\beta} & 0 & 0 \\ 0 & 0 & \varepsilon\beta & 0 \\ 0 & 0 & 0 & \frac{\varepsilon}{\beta} \end{bmatrix}. \quad (6)$$

Assuming a very short solenoid, its transfer matrix can be divided into two parts

$$R_{in} = \begin{bmatrix} 1 & 0 & 0 & 0 \\ 0 & 1 & k_{in} & 0 \\ 0 & 0 & 1 & 0 \\ -k_{in} & 0 & 0 & 1 \end{bmatrix}, \quad (7)$$

$$R_{out} = \begin{bmatrix} 1 & 0 & 0 & 0 \\ 0 & 1 & -k_{out} & 0 \\ 0 & 0 & 1 & 0 \\ k_{out} & 0 & 0 & 1 \end{bmatrix}. \quad (8)$$

The first part describes the entrance fringe field and the second part is the exit fringe field. If the beam has the same beam rigidity at the solenoid entrance (no foil inside solenoid) and exit k_{in} is equal to k_{out} ($k_{in}=k_{out}=k$). In here the focusing strength of the solenoid is

$$k = \frac{B}{2(B\rho)}. \quad (9)$$

B is the on-axis magnetic field strength and $B\rho$ is the beam rigidity. The beam matrix C_1 after the entrance fringe field k is found as

$$C_1 = \begin{bmatrix} \varepsilon\beta & 0 & 0 & -k\varepsilon\beta \\ 0 & \frac{\varepsilon}{\beta} + k^2\varepsilon\beta & k\varepsilon\beta & 0 \\ 0 & k\varepsilon\beta & \varepsilon\beta & 0 \\ -k\varepsilon\beta & 0 & 0 & \frac{\varepsilon}{\beta} + k^2\varepsilon\beta \end{bmatrix}. \quad (10)$$

The off-diagonal sub-matrices describe the correlations and the values of $\langle xy \rangle$ and $\langle x'y' \rangle$ are zero. In order to change the eigen-emittances, a non-symplectic transformation has to be integrated into the round-to-flat transformation section. The transformation through the solenoid is non-symplectic if the beam rigidity is abruptly changed in between the entrance and exit fringe fields, thus the beam properties are reset inside the solenoid. The non-symplectic transformation is accomplished for instance by changing the beam rigidity $B\rho$ in between the fringe fields from $(B\rho)_{in}$ to $(B\rho)_{out}$ through charge state stripping. Defining

$$\delta q := \frac{(B\rho)_{in}}{(B\rho)_{out}} \quad (11)$$

the exit fringe field transfer matrix changes to ($k_{in}=k$, $k_{out}=\delta qk$)

$$R'_{out} = \begin{bmatrix} 1 & 0 & 0 & 0 \\ 0 & 1 & -\delta qk & 0 \\ 0 & 0 & 1 & 0 \\ \delta qk & 0 & 0 & 1 \end{bmatrix}. \quad (12)$$

The focusing strength of the solenoid k is calculated from the unstripped charge state. The elements of the beam matrix C'_1 directly after the stripper foil inside of the solenoid but still before the exit fringe field are

$$C'_1 = \begin{bmatrix} \varepsilon\beta & 0 & 0 & -k\varepsilon\beta \\ 0 & \frac{\varepsilon}{\beta} + k^2\varepsilon\beta + \Delta\varphi^2 & k\varepsilon\beta & 0 \\ 0 & k\varepsilon\beta & \varepsilon\beta & 0 \\ -k\varepsilon\beta & 0 & 0 & \frac{\varepsilon}{\beta} + k^2\varepsilon\beta + \Delta\varphi^2 \end{bmatrix} \quad (13)$$

with stripping scattering effects on the angular spread being included. The parameter $\Delta\varphi^2$ is the scattering amount during the stripping process, and the stripper foil itself is modeled by increasing the spread of the angular distribution through scattering. After the stripper foil the beam passes through the exit fringe field with reduced beam rigidity and the beam matrix C'_2 after the exit fringe field becomes

$$C'_2 = \begin{bmatrix} \varepsilon_n R_n & ak\varepsilon_n \beta_n J_n \\ -ak\varepsilon_n \beta_n J_n & \varepsilon_n R_n \end{bmatrix} \quad (14)$$

where $a := \delta q - 1$ and

$$\varepsilon_n = \sqrt{\varepsilon\beta\left(\frac{\varepsilon}{\beta} + a^2k^2\varepsilon\beta + \Delta\varphi^2\right)}, \quad \beta_n = \frac{\beta\varepsilon}{\varepsilon_n}, \quad (15)$$

introducing the 2×2 sub-matrices R_n and J_n

$$R_n = \begin{bmatrix} \beta_n & 0 \\ 0 & \frac{1}{\beta_n} \end{bmatrix}, \quad J_n = \begin{bmatrix} 0 & 1 \\ -1 & 0 \end{bmatrix}. \quad (16)$$

The amount of eigen-emittance transfer scales with the longitudinal magnetic field strength and the beam rms sizes on the stripper. Inter-plane correlations are created and the rms emittances and eigen-emittances after the solenoid with stripper foil read

$$\varepsilon_{x,y} = \varepsilon_n, \quad \varepsilon_{1,2} = \varepsilon_n(1 \pm ak\beta_n). \quad (17)$$

The parameter t is introduced to quantify the inter-plane coupling. If t defined as

$$t = \frac{\varepsilon_x \varepsilon_y}{\varepsilon_1 \varepsilon_2} - 1 \geq 0 \quad (18)$$

is equal to zero, there are no inter-plane correlations and the beam is fully decoupled. After the solenoid exit fringe field, the t value can be calculated as

$$t = \frac{a^2k^2\varepsilon\beta}{\frac{\varepsilon}{\beta} + \Delta\varphi^2} \quad (19)$$

and the four-dimensional rms emittance is

$$\varepsilon_{4d} = \varepsilon_1 \varepsilon_2 = \varepsilon^2 + \varepsilon\beta\Delta\varphi^2. \quad (20)$$

The four-dimensional rms emittance increase is proportional to the beam sizes on the stripper foil. It is purely from scattering in the foil; it is not caused by the shift of beam rigidity inside the longitudinal magnetic field.

DECOUPLING SECTION

The simplest skew decoupling section only contains three skew quadrupoles with appropriate betatron phase advances in each plane. Let R_q be the 4×4 matrix corresponding to a certain arrangement of quadrupoles and drift spaces and assume that this channel is represented by an identity matrix in the x -direction and has an additional 90° phase advance in y -direction as in [5]

$$R_q = \begin{bmatrix} I_n & O_n \\ O_n & T_n \end{bmatrix}. \quad (21)$$

Here the 2×2 sub-matrices O_n , T_n and I_n are defined as

$$O_n = \begin{bmatrix} 0 & 0 \\ 0 & 0 \end{bmatrix}, \quad T_n = \begin{bmatrix} 0 & u \\ -\frac{1}{u} & 0 \end{bmatrix}, \quad I_n = \begin{bmatrix} 1 & 0 \\ 0 & 1 \end{bmatrix}. \quad (22)$$

If the quadrupoles are tilted by 45° the 4×4 transfer matrix can be written as

$$\bar{R} = R_r R_q R_r^T = \frac{1}{2} \begin{bmatrix} T_{n+} & T_{n-} \\ T_{n-} & T_{n+} \end{bmatrix}, \quad (23)$$

where

$$R_r = \frac{\sqrt{2}}{2} \begin{bmatrix} I_n & I_n \\ -I_n & I_n \end{bmatrix}, \quad T_{n\pm} = T_n \pm I_n. \quad (24)$$

The beam matrix C'_3 after the decoupling section is

$$C'_3 = \bar{R} C'_2 \bar{R}^T = \begin{bmatrix} \eta_+ \Gamma_{n+} & \zeta \Gamma_{n-} \\ \zeta \Gamma_{n-} & \eta_- \Gamma_{n+} \end{bmatrix}, \quad (25)$$

and the 2×2 sub-matrices $\Gamma_{n\pm}$ are defined through

$$\Gamma_{n\pm} = \begin{bmatrix} u & 0 \\ 0 & \pm \frac{1}{u} \end{bmatrix}, \quad (26)$$

with

$$\eta_{\pm} = \frac{\varepsilon_n}{2} \left(\frac{\beta_n}{u} + \frac{u}{\beta_n} \pm 2ak\beta_n \right), \quad (27)$$

and

$$\zeta = \frac{\varepsilon_n}{2} \left(-\frac{\beta_n}{u} + \frac{u}{\beta_n} \right). \quad (28)$$

Assuming that this beam matrix is diagonal, its x - y component vanishes

$$\zeta \Gamma_{n-} = O_n \quad (29)$$

solved by

$$u = \beta_n. \quad (30)$$

Suppose that the decoupling transfer matrix \bar{R} is able to decouple the two transverse planes of C'_2 . We still do not know how this transfer beam line looks in detail, but anyway we calculate the final rms emittances obtaining

$$\varepsilon_{x,y} = \frac{\varepsilon_n}{2} \left(\frac{\beta_n}{u} + \frac{u}{\beta_n} \pm 2ak\beta_n \right). \quad (31)$$

This idealized example serves illustrating the principle, and it may be accomplished with just three skew

quadrupoles. For a given solenoid strength k_0 , referring to the unstripped beam, the corresponding quadrupole gradients of the decoupling section are determined using a numerical routine, such that finally the rms emittances are equal to the eigen-emittances. If these optimized gradients are applied to remove inter-plane correlations produced by a different solenoid strength k_1 , the resulting rms emittances and eigen-emittances at the exit of the decoupling section are calculated to be

$$\varepsilon_{x,y} = \frac{\varepsilon_n(k_1)}{2} \left[\frac{\beta_n(k_1)}{\beta_n(k_0)} + \frac{\beta_n(k_0)}{\beta_n(k_1)} \pm 2ak_1\beta_n(k_1) \right] \quad (32)$$

and

$$\varepsilon_{1,2} = \varepsilon_n(k_1) [1 \pm ak_1\beta_n(k_1)] \quad (33)$$

with the parameter t

$$t = \frac{a^4 \varepsilon^2 \beta^2}{\left(\frac{\varepsilon}{\beta} + \Delta\varphi^2\right)\left(\frac{\varepsilon}{\beta} + a^2 k_0^2 \varepsilon \beta + \Delta\varphi^2\right)} \frac{(k_1^2 - k_0^2)^2}{4}. \quad (34)$$

In the same way the rms Twiss parameters of a beam coupled by k_1 but decoupled by $\bar{R}(k_0)$ are found from Equ. (25) as

$$\tilde{\alpha}_x = \tilde{\alpha}_y = 0, \quad \tilde{\beta}_x = \tilde{\beta}_y = \beta_n(k_0), \quad (35)$$

showing that the rms Twiss parameters after decoupling section do not depend on the coupling solenoid strength k_1 if the decoupling section was set assuming a coupling strength k_0 .

EMTEX beam line uses more elements than a single skew triplet because of finite apertures and gradients of a real experiment. Its decoupling section comprises a quadrupole triplet and a skew quadrupole triplet separated by a drift. The quadrupole gradients are optimized numerically from a numerical routine to remove the inter-plane correlations thus minimizing the horizontal (for instance) rms emittances to the lower of the eigen-emittances.

DYNAMICS SIMULATION

Fig. 2 illustrates the transverse emittance transfer and the multi-particle beam dynamics simulations have been done using the TRACK code [6].

In the first step we assume that the power supplies of the solenoid and the skew quadrupole triplet are turned off. This process is an ordinary stripping process and the eigen-emittances are equal to the rms emittances at the entrance and exit of this section. Due to the stripping, and the growth of eigen-emittances and rms emittances is unavoidable. It is the reference scenario to which the transverse rms emittance transfer scenario is to be compared.

In the latter case, the power supplies of the solenoid and the skew quadrupoles triplet are turned on. Once the beam enters the entrance fringe field maps of the solenoid, the eigen-emittances start to split gradually. After stripping, the exit fringe field maps of the solenoid is passed by the beam with reduced beam rigidity, thus overcompensating the previous eigen-emittance separation; the eigen-emittances diverge inside the solenoid and are preserved

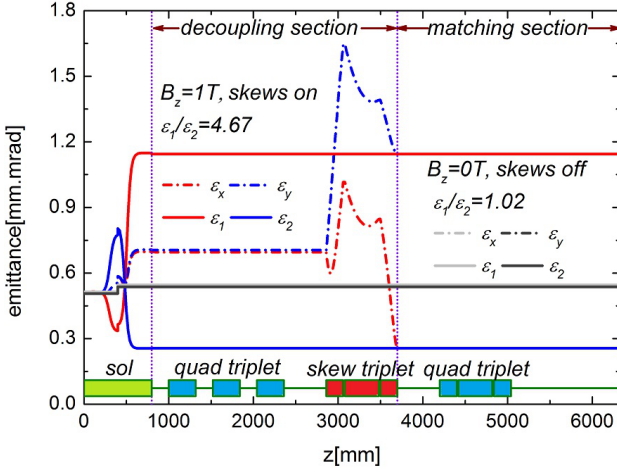


Figure 2: Evolution of the rms emittances and eigen-emittances along the EMTEX beam lines for two cases.

afterwards. Along the decoupling skew quadrupole triplet the rms emittances are made equal to the separated eigen-emittances. Compared to the reference scenario, the final horizontal rms emittance is reduced significantly. Emittance transfer is non-symplectic and the amount of transfer can be controlled by the solenoid field strength and the beam size on the stripping foil.

DECOUPLING CAPABILITY ANALYSIS

Final eigen-emittances and rms emittances at the exit of the skew quadrupole triplet calculated using Equ. (23) and those obtained from tracking through EMTEX beam line are compared in Fig. 3.

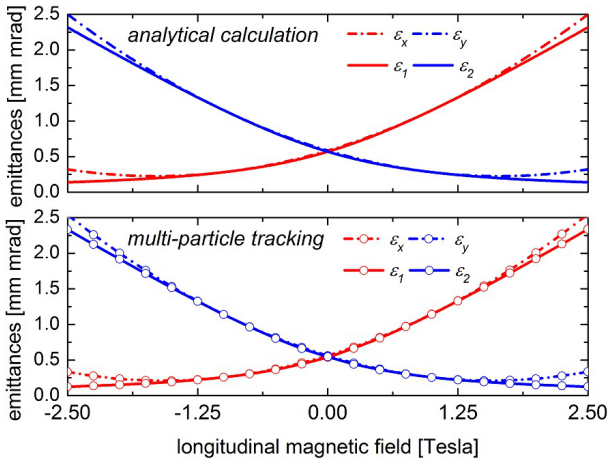


Figure 3: Eigen-emittances and rms emittances calculated by analytical method based on the decoupling matrix of Equ. (23) and by multi-particle tracking through the EMTEX beam line.

The remarkable result is that both decoupling matrices work effectively for a wide range of longitudinal magnetic field values, i.e. the beam is well decoupled for a wide range of longitudinal magnetic fields around the gradients

the quadrupoles have been optimized for. Additionally, in both cases the decoupling performance is independent from the sign of k_1 as suggested by Equ. (34) and weakly depended on $(k_1 - k_0)$. This behavior simplifies the decoupling significantly as re-adoption of gradients to the solenoid field can be skipped within a reasonable range of solenoid fields. It provides a single-knob tool to partition the horizontal and vertical beam rms emittances. EMTEX will use the solenoid field strength to control the amount of eigen-emittance change, and the decoupling gradients must be re-adapted to the specific solenoid field strength.

MATCHING CAPABILITY ANALYSIS

Another convenient feature of EMTEX, which can be explained for the generic case of decoupling according to Equ. (23), seems to manifest as a general rule in numerical matrix as well as in tracking calculations. Its generality we cannot explain for the time being: the shape of the transverse beta-functions after the decoupling section does not practically depend on the solenoid field strength. In other words, the two transverse rms ellipses after decoupling are just changed in size through the solenoid field; their orientation and shape remains unaffected by the solenoid strength. This matching capability of EMTEX is illustrated in Fig. 4.

DECOUPLING IN THE GENERAL CASE

In order to fully understand the decoupling properties of generic beam line, a procedure being illustrated in Fig. 5.

Suppose a there is any arbitrary beam line M_D that provides decoupling, and this beam line includes x - y coupling linear elements. We prolong M_D by a beam line represented by the matrix

$$A = \begin{bmatrix} A_x & O_n \\ O_n & A_y \end{bmatrix}. \quad (36)$$

with the 2×2 sub-matrices A_x and A_y , and A must not include any x - y coupling element. The resulting total beam line \bar{R} is the product AM_D , then we have non-coupling line $A = \bar{R}M_D^{-1}$. As shown above, at the exit of \bar{R} the properties hold. From the exit of \bar{R} the Twiss parameters α , and β (in both planes) are transported backwards to S_D by applying A^{-1} being aware that α , and β do not depend from the fringe strength. As A does not include any x - y coupling element, neither does A^{-1} . Accordingly, the back-transformed Twiss parameters at S_D also do not depend on the fringe strength. The same way the invariance of the Twiss parameters w.r.t. the fringe strength is kept through the back-transportation by A^{-1} , the weak dependence of $t(k_1)$ is back-transported and preserved through A^{-1} . Since A^{-1} is non-coupling, it preserves t value. In other words, the properties at the exit of \bar{R} are preserved during back-transportation by A^{-1} . As a consequence the properties hold also at the exit of the arbitrarily chosen decoupling beam line M_D .

These arguments are summarized in the formula

$$M_D = A^{-1}\bar{R} \quad (37)$$

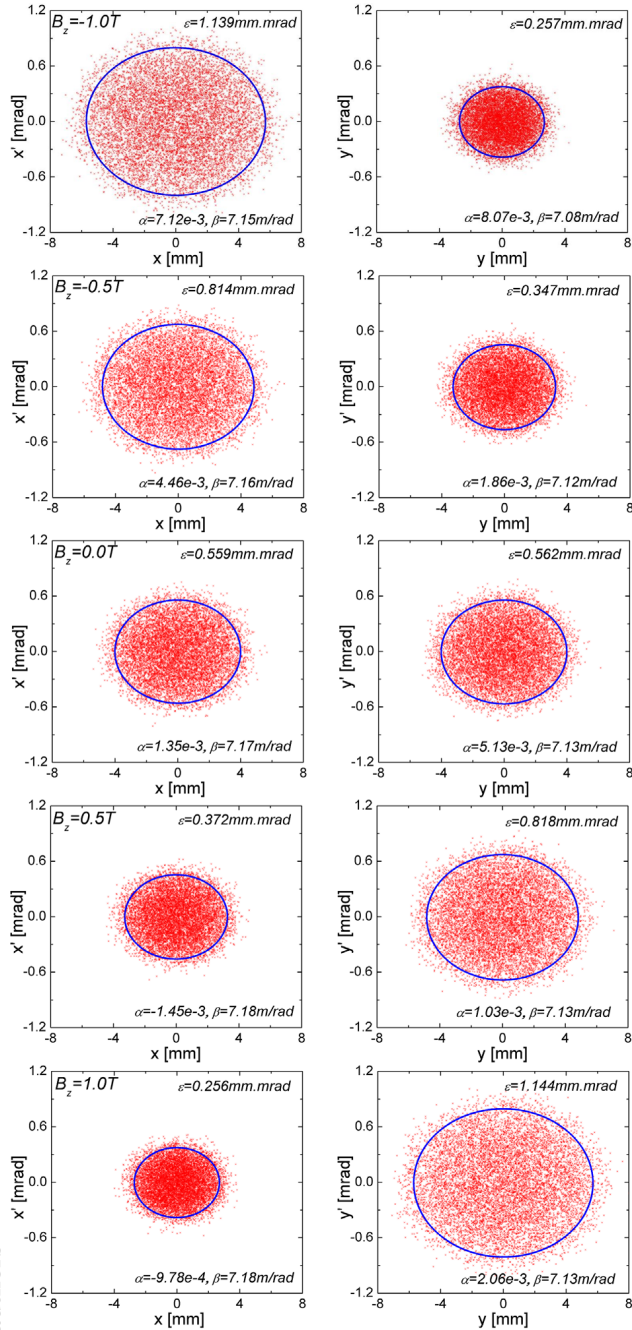


Figure 4: The transverse emittance portraits at the exit of the beam line for different solenoid field strengths. The gradients of the quadrupoles and skew quadrupoles are constant. The rms Twiss parameters do not depend on the solenoid field strength.

\bar{R} has the properties, which has been derived in the previous section. The matrix A^{-1} does not change them since it is non-coupling. As a consequence, the properties are also intrinsic properties of M_D [7].

CONCLUSION AND OUTLOOK

A beam line for demonstration of round-to-flat transformation of an initially uncoupled ion beam was presented. The net effect on the beam is a non-symplectic transfor-

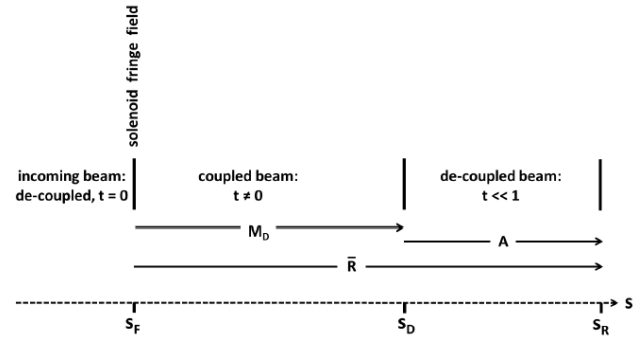


Figure 5: Extension of the decoupling features of the generic beam line \bar{R} to any decoupling beam line M_D . S_F denotes the location of the initially coupling stand-alone solenoid fringe field. The arbitrary decoupling beam line M_D ends at S_D , and the generic beam line R ends at S_R . The beam line A does not include any x - y coupling element.

mation creating inter-plane coupling, being removed afterwards along a beam line from one regular quadrupole triplet and one skew quadrupole triplet. Angular scattering during stripping was included.

The beam line decoupling performance was found to be very stable w.r.t. the magnetic field strength of the solenoid, i.e. the same decoupling gradients can be applied for a wide range of solenoid fields without relevant reduction of the decoupling performance. After the beam is decoupled its rms Twiss parameters $\alpha_x, \beta_x, \alpha_y, \beta_y$ do not practically depend on the solenoid field strength that created the coupling.

REFERENCES

- [1] A.J. Dragt, Phys. Rev. A **45**, (1992).
- [2] L. Groening, Phys. Rev. ST Accel. Beams **14**, 064201 (2011).
- [3] W. Barth et al., Proc. XXIV Linac Conf., p. 175, (2008).
- [4] C. Xiao et al, Phys. Rev. ST Accel. Beams **16**, 044201 (2013).
- [5] K.J. Kim et al, Phys. Rev. ST Accel. Beams **6**, 104002 (2003).
- [6] <http://www.phy.anl.gov/atlas/TRACK/>
- [7] L. Groening, <http://arxiv.org/abs/1403.6962v1>